Carrier dynamics in conducting polymers: Case of PF6 doped Polypyrrole

Romijn, I.G.; Hupkes, H.J.; Martens, H.C.F.; Brom, H.B.; Mukherjee, A.; Menon, R.

Carrier Dynamics in Conducting Polymers: Case of PF_6 Doped Polypyrrole

I. G. Romijn, H. J. Hupkes, H. C. F. Martens, and H. B. Brom
Kamerlingh Onnes Laboratory, Leiden University, P.O. Box 9504, 2300 RA Leiden, The Netherlands

A. K. Mukherjee and R. Menon
Indian Institute of Science, Department of Physics, Bangalore, India
(Received 9 January 2003; published 29 April 2003)

The carrier dynamics in PF_6 doped polypyrrole has been probed by dielectric spectroscopy (from 10^{-4} to 4 eV), down to 4.2 K. The phase-sensitive sub-THz data have assisted to resolve the discrepancies in Kramers-Kronig analysis in earlier studies. Even in metallic samples, just 1% of the carriers are delocalized, at 300 K; the fraction drops down considerably as a function of disorder, carrier density, and temperature. This subtle metallic feature and the anomalies in carrier dynamics are attributed to coherent and incoherent transport between short conjugated segments.

DOI: 10.1103/PhysRevLett.90.176602 PACS numbers: 72.80.Le, 71.20.Rv, 72.20.Ee, 73.61.Ph

The charge carrier dynamics and metallic state in low-dimensional systems such as conducting polymers [1–5], carbon nanotubes [6,7], charge-transfer salts [8], and high-T_c cuprates [9] have several anomalies like a Drude peak at very low energies, a second plasma frequency at higher energies, and time constants of the order of few picoseconds. Especially in doped conducting polymers, the situation is quite complicated due to the coexistence of crystalline and amorphous regions in the systems, which has lead to so-called heterogeneous and homogeneous models to interpret the experimental data with ambiguous results [1–3,10–12]. The typical parameters that are involved in determining the electronic properties of conducting polymers are the crystalline coherence length (a few nanometers), volume fraction of crystallinity (~50%), doping level (typical carrier densities 10^{21} cm^{-3}), interchain transfer integral (and bandwidth), Coulomb correlations, and random disorder potentials, which are all estimated to be around 0.1 eV. Recently intergrain resonant tunneling through strongly localized states in the amorphous media between the crystalline polymeric islands was considered to play a role as well [13]. Other groups [5,14] stressed that disorder and Coulomb interactions should be compared to the energy scale of interchain charge transfer. The usual experimental technique to investigate the carrier dynamics in such a metallic system is the high frequency reflectance (5 meV to 4 eV) and then to follow Kramers-Kronig (KK) analysis (abbreviated KKA) with appropriate extrapolations at high and low frequencies. However, KKA on quite similar reflectance data in metallic conducting polymers, by various groups, has led to conflicting results. These differences appear mainly to be due to the uncertainty in the extrapolations. We show that phase-sensitive sub-THz data are essential for unambiguous KKA results at low frequencies. Hence the sub-THz data along with Fourier-transform infrared (FTIR) and ultraviolet-visible (UV-VIS) data (0.04 meV–3.5 eV) on PF_6 doped polypyrrole (PPy) samples, in metallic and critical regime of metal-insulator transition (MIT), helps to resolve the inconsistencies in earlier work. Moreover, the data analysis indicates that the carrier dynamics in such complex systems involve both coherent and incoherent transport via the conjugated polymer segments (i.e., short chains of undisturbed π electrons) in amorphous regions, which are typically below 1 nm in size. The tunnel transport via this rather small length scale plays a crucial role in the carrier dynamics, and this suggests that the distinction between heterogeneous and homogeneous models for PPy is just a matter of semantics.

Among the various conducting polymers, PF_6-doped PPy is one of the best studied systems, in which it is possible to fine tune the MIT as a function of carrier density or disorder, as in the case of doped silicon. Free-standing films of PPy doped with PF_6 were prepared electrochemically as described in detail elsewhere [1,3]. We measured $\sigma_{DC}(T)$ and use the reduced activation energy $d\ln(\sigma)/d\ln(T)$ of the samples to determine their position relative to the MIT. The transport properties in the range of 10–800 GHz (0.04–3.3 meV) were studied by means of complex transmission spectroscopy [15], which allows the determination of $\epsilon^*(\omega) = \epsilon_0[\epsilon_1(\omega) + i\epsilon_2(\omega)] = \epsilon_0\epsilon_1(\omega) + i\sigma_1(\omega)/\omega$ directly (in the following $\epsilon \equiv \epsilon_1$ and $\sigma \equiv \sigma_1$). The high frequency reflection data were obtained using a Bruker FTIR (5 meV to 0.5 eV) and a Perkin-Elmer UV/VIS spectrometer (0.5 to 3.5 eV). The analysis of two relevant PPy samples will be completely described. PPy_M is on the metallic side of the MIT (nonzero σ_{DC} at $T = 0$), while PPy_C is on the critical edge ($\sigma_{DC} \propto T$)—both samples have the same doping but differ in polymerization temperature [5]. PPy_D is partially dedoped and in the insulating regime. The reflection data for PPy_M, PPy_C, and PPy_D at 300 K are shown in Fig. 1(a); reflection in the GHz regime is calculated from the measured σ and ϵ. Values of $\epsilon(\omega)$ and $\sigma(\omega)$ over the whole

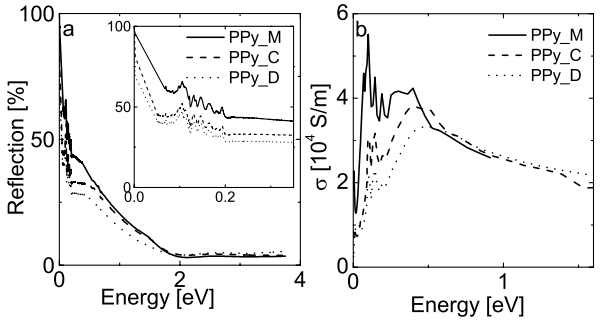

FIG. 1. (a) IR and UV/VIS reflection of three PF_6 doped PPy samples at 300 K. The overall features are similar (b) $\sigma_1(\omega)$ derived from (a) according to the procedure in the text.

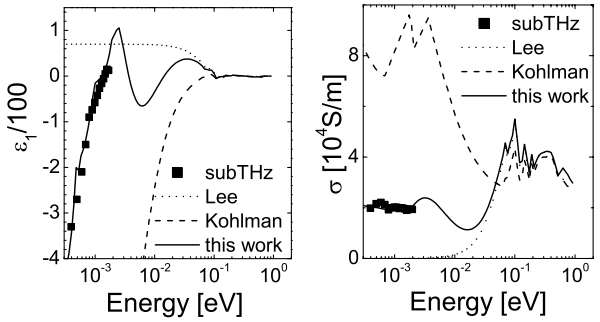

FIG. 2. Three outcomes of KKA for PPy_M at 300 K: the dotted and dashed lines mimic the outcomes of, respectively, Lee *et al.* and Kohlman *et al.* For the full line the sub-THz ϵ and σ data (black squares) are used as boundary conditions.

frequency range are calculated from the reflectance $R(\omega)$ and phase $\theta(\omega)$, where the latter is obtained via KKA $\theta(\omega_0) = (\omega_0/\pi)\int_0^\infty \ln[R(\omega)/R(\omega_0)]/[\omega_0^2 - \omega^2]d\omega$, with appropriate extrapolation schemes at high and low frequencies [16]. The directly measured values for $\epsilon(\omega)$ and $\sigma(\omega)$ below 800 GHz are used as an extra boundary condition.

Although our reflection data are similar to those reported earlier, the differences in $\epsilon(\omega)$ and $\sigma(\omega)$ are significant. For PPy in the metallic regime Lee *et al.* [3,12] measured the reflectivity down to 5 meV. From their KKA, at low frequencies ϵ turned out to be around 20 and σ shows a tendency to approach zero; at high frequencies σ peaked around 0.6 eV while ϵ showed a small negative dip. Using the homogeneous disorder model, Lee *et al.* found a plasma frequency $\sim$1.8 eV and a scattering time $\sim 3.5 \times 10^{-15}$ s. Kohlman *et al.* [2] obtained similar reflection data, but after KKA got significant different results for σ and ϵ. With increasing ω, ϵ went from large negative to positive values at 0.03 eV, crossed again around 0.1 eV and became positive once more around 1 eV. Within the heterogeneous model [13], the interpretation is as follows. At high ω, ϵ is negative due to electrons delocalized over the "metallic" islands. These carriers have small scattering times ($\sim 10^{-15}$ s) and large plasma frequency ($\sim$2 eV). When ω is smaller than the time for diffusive transport across the grain, the islands start behaving like dielectric dipoles: ϵ turns positive and σ decreases. When the probing frequency ω becomes smaller than the average intergrain hopping/tunnel rate, electrons will be able to tunnel from one grain to the other and the system becomes metallic again with negative ϵ. Also Chapman *et al.* got similar reflection data (here ϵ remains positive down to 7.5 meV), which were shown to be compatible with a heterogenous model [4,11,17]. We could mimic these outcomes by ignoring our sub-THz data and using different extrapolations at low frequencies. For example, for Lee's data it was sufficient to keep the reflectance constant at $\approx$60% [18], while for Kohlman the reflectance was extrapolated to 100% at low frequency. These calculations, together with our new results, are shown in Fig. 2. It shows KKA to be very sensitive to small changes, and knowledge of phase information in the sub-THz regime to be essential.

A complete analysis for PPy_M and PPy_C at three different temperatures is shown in Fig. 3. Our results at high energy values, where we mainly see localized carriers, agree with the findings of Lee *et al.* [3]. The peaked σ at high ω can be fitted with either a localized Drude model [3], a heterogeneous model [11,17], or a simple Lorentz oscillator for the localized electrons (see below). At energies below 0.1 eV, we mainly see the delocalized carriers as indicated by the negative value of ϵ [19], which were absent in the analysis of both Lee *et al.* [3] and Chapman *et al.* [4], but present in that of Kohlman *et al.* [2]. The main difference with the latter is that the energies of the ϵ transitions through zero at E_1 and E_2 with $E_1 < E_2$ are 1 order of magnitude lower in our analysis with the proper low ω input. It gives for PPy_M at 300 K magnitudes of the positive and negative peak in ϵ around 100; in the analysis of Kohlman *et al.* this is an order of magnitude lower [2,13], and therefore not clearly visible in Fig. 2.

Using the sum rule $\int_0^\infty \omega\epsilon_2(\omega)d\omega = (\pi/2)(N_e e^2)/(\epsilon_0 m)$ [16,20] we estimated N_e/m. Interpretation of these values has to be done with care, especially when restricted energy intervals are selected and the effective mass has to be introduced [16]. The values of N_e/m, obtained after integration to 4 eV, for PPy_M and PPy_C (the same within the error bar) are slightly higher than for PPY_D. Using the free electron mass, the number of electrons per PPy monomer equals 0.68 ± 0.01. Similar values are published in the literature [3]. The presence of delocalized or weakly localized carriers clearly show up below 0.01 eV and hence their number can be estimated by integrating the σ data up to 0.02 eV. When we separate this contribution from the strongly localized carriers visible above 0.1 eV the results are as follows. At 300 K for PPy_M at most 1% of the carriers is delocalized, and this number drops to 0.1% for PPy_C, at 300 K. When going to lower energies or temperatures, the number of delocalized carriers decreases further by an order of magnitude.

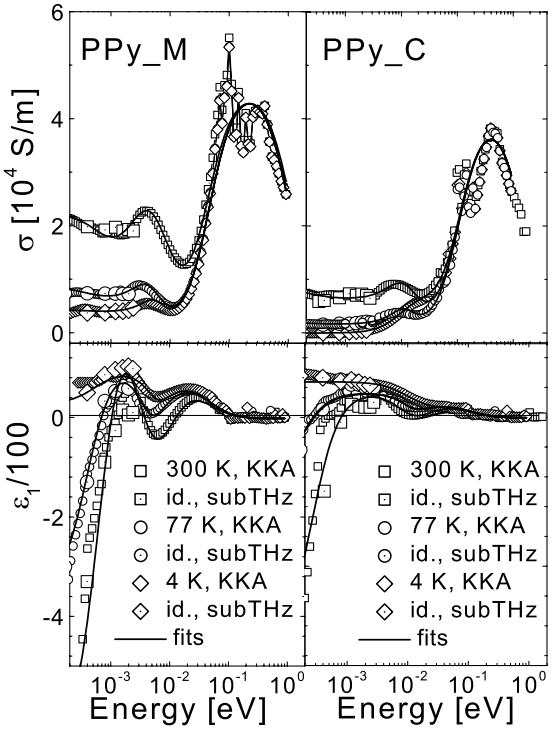

FIG. 3. $\epsilon_1(\omega)$ and $\sigma_1(\omega)$ for PPy_M and PPy_C at various T. Small symbols are the KK data, large symbols the subTHz-data used as boundary conditions (see also Ref. [5]). Full lines are fits with the model, see text [19].

Before going to a full quantitative analysis of the data, we like to draw the attention to a few essential differences between PPy on the one side and other metallic conjugated polymers such as polyacetylene (PAc) and polyaniline (PAN) on the other. PPy is not as crystalline as PAc or PAN. The approximate crystalline coherence lengths in PPy, PAN, and PAc are 2, 5, and 10 nm, respectively. The crystalline volume fraction in PPy is around 50% [21,22]. Because of the smaller crystalline regions in PPy compared to PAN the scattering time of the electrons will be of the same order of magnitude as the grain crossing time $\sim 10^{-14}$ s, and hence the meaning of metallic islands is marginal as it has the dimensions of a chain segment of a few monomers [23]. For PPy to be metallic the transmission coefficients for tunneling between island (chain segments) has to be larger than a critical value, which is estimated to be $\approx 10^{-2}$ [13]. For direct tunneling between adjacent grains, the transmission coefficient can be written as $\exp(-2L/\xi)$, with L the distance between the separate crystalline regions, and ξ the electron localization length. For samples with 50% crystallinity L is about the grain size (2 nm for PPy) and $\xi \approx 1$ nm [13]. This implies that contrary to PAN, for PPy direct tunneling remains relevant. The coherent tunnel rate (due to direct and resonant [13] tunneling) will be denoted by $1/\tau_c$.

For doped PPy with conjugated polymer segments being the metallic islands, various characteristic frequencies should be taken into account while describing the dynamics of delocalized carriers: in decreasing order the plasma frequency $\omega_{p,s}$ and the scattering rate $1/\tau_s$ of the electrons in the segments, and the coherent electron tunneling rate $1/\tau_c$. Parallel to the coherent contribution to the conduction, phonon assisted incoherent transport between the segments will contribute as well (characteristic time constant τ_i). The complex conductivity $\sigma(\omega)$ can be written $\sigma(\omega)^{-1} = \sigma_s(\omega)^{-1} + (a\hbar/e^2)[g_i(\omega) + g_c(\omega)]^{-1}$ with $a\hbar/e^2$ a conductivity unit appropriate to the intersegment distance a. The conductivity on the segments $\sigma_s(\omega) = \sigma_{s,0}/(1 + i\omega\tau_s)$ with $\sigma_{s,0} = \epsilon_0\omega_{p,s}^2\tau_s$, while the transmission coefficient for the coherent transport channel between chain segments equals $g_c = g_{c,0}/(1 + i\omega\tau_c)$ [13,24]. The incoherent transmission coefficient at frequencies much lower than the phonon Debye frequency is $g_i = g_{i,0}(1 + i\omega\tau_i)$ [26]. Kaiser *et al.* used a similar formula [4,17] to fit the dielectric data at high energy ($\sim$eV). In contrast, the carriers described by the equations here give their contribution at relatively low energies (<0.1 eV). In addition, the vast majority of charges is localized and only involved in the contribution at high energy, which is well described by a Lorentz oscillator $\epsilon_{\rm loc}/\epsilon_0 = 1 + (Ne^2/m\epsilon_0)(\omega_0^2 - \omega^2 + i\omega\Delta)^{-1}$ with $\omega_0 = 0.22$ eV and $\Delta = 1.2$ eV and $N = 2.7 \times 10^{27}\,\mathrm{m}^{-3}$ for sample PPy_M and $\omega_0 = 0.4$ eV and $\Delta = 1.6$ eV and $N = 2.9 \times 10^{27}\,\mathrm{m}^{-3}$ for sample PPy_C. From the fits it appears that these values hardly change with temperature. Both parameters, the resonance frequency ω_0 and the damping constant (inverse scattering time) Δ, are properties of bounded (localized) charges in the polymer matrix. Interestingly, Δ is of the order of the energy uncertainty of a "free" electron confined in a potential well of a few nm.

The values of the parameters of the fit for the delocalized and weakly localized carriers in Fig. 3 are given in Table I. Going from 0.1 eV down, the first negative contribution in ϵ and the rise in σ at 0.1 eV are caused by the conduction within the chain segment. The prefactor $\sigma_{s,0} = \epsilon_o\omega_{p,s}^2\tau_s$ goes down with T while τ_s rises. It implies that the number of carriers ($\omega_{p,s}$) in the segment that participates in the transport process decreases and hence were partly thermally activated. The decreasing phonon scattering may cause τ_s to rise at lower T. Comparing PPy_C with PPy_M, we see that in PPy_C both τ_s and $\sigma_{s,0}$ are smaller, since the size of the metallic segments and the number of carriers are decreased due to the increase in disorder. The incoherent channel causes ϵ to become positive and σ to drop around 10^{-2} eV. The coherent channel (tunneling between the conjugated segments) gives the Drude contribution at $\hbar\omega < 10$ meV. Looking at $\sigma_{c,0}$ and $\sigma_{i,0}$, we see the number of carriers participating in coherent and incoherent transport both decrease with T, but those participating in incoherent transport become relatively more important at low temperature. In the case of PPy_C at 77 K, the contribution of the coherent channel is significantly less than that of the incoherent channel, producing a positive ϵ at low

TABLE I. Transport parameters obtained from the fits in Fig. 3. σ is S/m and τ in ps. Errors are about 10% for σ and 20% for τ. $\sigma_{c,0}$ and $\sigma_{i,0}$ are short for $(a\hbar/e^2)g_{c,0}$ and $(a\hbar/e^2)g_{i,0}$. To fit PPy_C at 4 K the segment Drude contribution has to be replaced by a Lorentz oscillator (localized carriers) with $\omega_0 \sim 0.02$ eV and width 0.05 eV.

Sample	T	$\sigma_{s,0}$	$\sigma_{c,0}$	$\sigma_{i,0}$	τ_s	τ_c	τ_i
PPy_M	300 K	2.7×10^4	1.4×10^5	5.2×10^4	0.46	17	1.7
	77 K	1.2×10^4	1.5×10^4	1.5×10^4	0.83	17	1.7
	4 K	0.85×10^4	1.4×10^3	7×10^3	1.04	17	1.3
PPy_C	300 K	1.1×10^4	1.6×10^4	1.6×10^4	0.25	25	0.83
	77 K	5.0×10^3	909	2.5×10^3	0.32	25	1.2
	4 K	(5.0×10^3)	...	...	(0.1)	...	...

frequencies. The T independence of $1/\tau_c$ is determined by the energy levels and the wave functions involved in the coherent charge transfer and its low value is due to the small tunnel rate. The value of $1/\tau_i$ is comparable to phonon frequencies as is typical for phonon-mediated incoherent (hopping) transport.

Finally, the present results are compared to earlier work by Martens *et al.* [5], who attempted a simple Drude analysis of the data below 2 meV with one free parameter: the density of states over the effective mass g/m^*. It was observed that g/m^* increases from $10^{-2}/\mathrm{ring\,eV\,m_e}$ for PPy_C to $10^{-1}/\mathrm{ring\,eV\,m_e}$ for PPy_M, at 300 K. Application of the sum rule showed that only about 1% of the PPy monomers participates in band conduction. In the (small dispersion) band the distance between energy levels is estimated to be of the order of 10 meV, similar to the energy splitting in the chain segment [24,25]. Hence for PPy M the value of $g(E)$ will be of the order of 1 state per 10 meV per 100 rings, or $g(E) = 1/\mathrm{ring\,eV}$. The experimental value for g/m^* can be obtained by inserting an effective mass of at least a few times m_e, which seems reasonable in view of the small bandwidth.

In summary, we have shown that phase-sensitive sub-THz data are a crucial ingredient for the consistent analysis of optical reflectance data by the KK method. Especially, in the case of disordered low-dimensional systems such as conducting polymers, charge carrier dynamics is dominated by the contributions at low energies, which can be probed only by sub-THz complex dielectric spectroscopy. For PPy the low-energy carrier dynamics is determined by the combination of coherent and incoherent transport channels between conjugated chain segments, where the coherent channel gives rise to the low-energy structure and negative value of ϵ, and the unusually long values of τ follow from the small coherent tunnel rate.

We acknowledge fruitful discussions with Kwanghee Lee, Vladimir Prigodin, and Alan Kaiser. This work was financially supported by FOM-NWO.

[1] C. O. Yoon *et al.*, Phys. Rev. B **49**, 10 851 (1994).
[2] R. S. Kohlman *et al.*, Phys. Rev. Lett. **74**, 773 (1995); **77**, 2766 (1996); **78**, 3915 (1997).
[3] K. Lee *et al.*, Phys. Rev. B **52**, 4779 (1995); Adv. Mater. **10**, 456 (1998).
[4] B. Chapman *et al.*, Phys. Rev. B **60**, 13 479 (1999).
[5] H. C. F. Martens *et al.*, Phys. Rev. B **63**, 073203 (2001); **64**, R201102 (2001); **65**, 079901 (2002).
[6] A. Ugawa *et al.*, Phys. Rev. B **60**, R11 305 (1999).
[7] O. Hilt *et al.*, Phys. Rev. B **61**, R5129 (2000).
[8] V. Vescoli *et al.*, Science **281**, 1181 (1998).
[9] S. Lupi *et al.*, Phys. Rev. B **62**, 12418 (2000).
[10] R. Menon *et al.*, in *Handbook of Conducting Polymers* (Marcel Dekker, New York, 1998), 2nd ed.
[11] A. B. Kaiser, Adv. Mater. **13**, 927 (2001); Rep. Prog. Phys. **64**, 1 (2001).
[12] K. Lee and A. J. Heeger, Synth. Met. **128**, 297 (2002).
[13] V. N. Prigodin and A. J. Epstein, Synth. Met. **125**, 43 (2002).
[14] Y. Kieffel *et al.*, Synth. Met. **135–136**, 325–326 (2003).
[15] J. A. Reedijk *et al.*, Rev. Sci. Instrum. **71**, 478 (2000).
[16] F. Wooten, *Optical Properties of Solids* (Academic Press, New York, 1972).
[17] A. B. Kaiser *et al.*, Synth. Met. **117**, 67 (2001).
[18] Lee *et al.* used the Hagens-Rubens extrapolation at low frequencies.
[19] The decrease of ϵ at low ω has to be accompanied by an increase of σ. Since the downturn of ϵ occurs at $\omega_p \sim$ meV the increment in $\sigma = \omega_p^2 \tau$ is a few 100 S/m, which is less than 10% of the total σ_{DC}.
[20] R. Kubo, J. Phys. Soc. Jpn. **12**, 570 (1957).
[21] J. P. Pouget *et al.*, Synth. Met. **65**, 131 (1994).
[22] Y. Nogami *et al.*, Synth. Met. **62**, 257 (1994).
[23] A 50% presence of crystalline regions does not imply a crystalline percolating path; compare with the high metal fillings in nonmetallic cermets.
[24] The transfer integral between polymer segments equals the level splitting in the delocalized region—for a nm particle around 10 meV [25].
[25] W. P. Halperin, Rev. Mod. Phys. **58**, 533 (1986).
[26] H. Böttger and V.V. Bryksin, *Hopping Conduction in Solids* (Akademie-Verlag, Berlin, 1985).